



Thermo-hydraulic design of a horizontal shell and tube condenser for methanol condensation

Diseño térmico-hidráulico de un condensador de tubo y coraza horizontal para la condensación de metanol

Amaury Pérez Sánchez ¹ * ; Yerelis Pons García ² , Daynel Basulto Pita ³ , Elizabeth Ranero González ⁴ & Eddy Javier Pérez Sánchez ⁵

Received: 08/08/2024 – Accepted: 23/11/2024 – Published: 01/01/2025

Research
Articles



Review
Articles



Essay
Articles



* Author for correspondence.



Abstract.

Shell and tube condensers are considered to be a significant part of refrigeration and power plants systems, as well as other petrochemical applications where the heat exchangers are usually employed. This article presents the thermo-hydraulic design of a one shell pass: two tube passes (1-2) horizontal shell and tube heat exchanger to condense a stream of pure methanol vapours using chilled water as a coolant. Several design parameters were calculated such as the heat transfer area (119.33 m²); the number of tubes (285); the shell internal diameter (800.56 mm) and the overall heat transfer coefficient (618.47 W/m².K). The calculated heat duty for this heat exchange service was of 8,272.5 kW, while the required flowrate for chilled water was of 151.59 kg/s. The calculated pressure drops for the condensing methanol and chilled water streams were 7,372.55 Pa and 84,289.69 Pa respectively, which are below the maximum limit values set by the process. The designed 1-2 shell and tube condenser was of pull-through floating head type, with a baffle cut of 45% and a baffle spacing equal to the shell internal diameter.

Keywords.

Heat Exchanger Area, Methanol Condensation, Pressure Drop, Shell And Tube Condenser, Thermo-Hydraulic Design

Resumen.

Los condensadores de tubo y coraza están considerados ser una parte significativa de los sistemas de refrigeración y plantas de potencia, así como de otras aplicaciones petroquímicas donde los intercambiadores de calor son usualmente empleados. Este artículo presenta el diseño térmico-hidráulico de un intercambiador de calor de tubo y coraza horizontal de un paso por la coraza y dos pasos por los tubos (1-2) para condensar una corriente de vapores de metanol puro usando agua fría como agente de enfriamiento. Varios parámetros de diseño fueron calculados tales como el área de transferencia de calor (119,33 m²); el número de tubos (285); el diámetro interno de la coraza (800,56 mm) y el coeficiente global de transferencia de calor (618,47 W/m².K). La carga de calor calculada para este servicio de transferencia de calor fue de 8 272,5 kW mientras que el caudal requerido de agua fría fue de 151,59 kg/s. Las caídas de presión calculadas para las corrientes de metanol condensante y agua fría fueron 7 372,55 Pa y 84 289,69 Pa respectivamente, las cuales están por debajo de los valores límites máximos fijados por el proceso. El condensador de tubo y coraza 1-2 diseñado fue del tipo cabezal flotante, con un corte del deflector de 45 % y un espaciado del deflector igual al diámetro interno de la coraza.

Palabras clave

Área De Intercambio De Calor, Condensación De Metanol, Caída De Presión, Condensador De Tubo Y Coraza, Diseño Térmico-Hidráulico

1. Introduction

Transfer of heat from one fluid to another is an important operation for most of the chemical industries. The most frequent application of heat transfer is the design of heat transfer equipment to exchange heat from one fluid to another fluid. Such devices for effective transfer of heat are commonly named heat exchanger.

Heat exchangers are based on the principle of heat transfer taking place between the higher temperature fluid and the lower temperature fluid. Heat exchangers operate by permitting the first fluid at a higher temperature to interact with the second fluid either directly or indirectly at a lower temperature. This allows heat to transfer from the first to the second fluid, resulting in a reduction in the second fluid's

temperature and an increase in the first fluid's temperature. Depending on whether heating or cooling is necessary, heat is transferred towards or away from the given system [1].

Typical applications include heating or cooling of a fluid stream of interest and evaporation or condensation of single- or multicomponent fluid streams. In other applications, the objective may be to recover or reject heat, or sterilize, pasteurize, fractionate, distill, concentrate, crystallize, or control a process fluid. In most heat exchangers, heat transfer between fluids takes place through a separating wall or into and out of a wall in a transient manner. In various heat exchangers, the fluids are separated by a heat transfer surface, and ideally, they do not mix or leak [2].

¹ University of Camagüey; Faculty of Applied Sciences; amaury.perez84@gmail.com; <https://orcid.org/0000-0002-0819-6760>; Camagüey; Cuba.

² University of Camagüey; Faculty of Applied Sciences; yerelis.pons@reduc.edu.cu; <https://orcid.org/0009-0003-0440-1784>; Camagüey; Cuba.

³ Center of Genetic Engineering and Biotechnology of Camagüey; Department of Production; daynel.basulto@cigb.edu.cu; <https://orcid.org/0009-0005-1629-8846>; Camagüey; Cuba.

⁴ University of Camagüey; Faculty of Applied Sciences; elizabeth.ranero@reduc.edu.cu; <https://orcid.org/0000-0001-9755-0276>; Camagüey; Cuba.

⁵ Company of Automotive Services S.A.; Commercial Department; eddy.perez@reduc.edu.cu; <https://orcid.org/0000-0003-4481-1262>; Ciego de Ávila, Cuba.

The heat exchangers are classified according to the transfer process, number of fluids, degree of surface compactness, construction features, flow arrangements and heat transfer mechanisms. Heat exchangers are extensively used in many engineering applications such as power engineering, petroleum refining, refrigeration, air conditioning, food industry, and biotechnological and chemical process industries [3].

Among the different types of heat exchangers, shell and tube heat exchangers (STHE) are the most common used in industry. They are relatively easy to manufacture and have multipurpose application potentials for gaseous and liquid media in large temperature and pressure ranges [3], with operating temperatures of - 20 °C to over 500 °C, maximum operating pressure of 600 bar and diameters ranging from 60 to over 2,000 mm [4]. According to [5] the shell and tube heat exchanger is used when a process requires large amounts of fluids to be heated (or vaporized) or cooled (or condensed), while due to their design, they offer a large heat transfer area and provide high heat transfer efficiency.

The main components of a STHE are identified in Figure 1, showing a 1-2 heat exchanger, that is, a heat exchanger with one shell-side pass and two tube-side passes. The tube-side fluid enters the heat exchanger from the tube fluid inlet (1) into front-end head (11) and from there into the tubes (4). The tube fluid exits the tubes of the first pass into the rear-end head (6), continues back into the second tube-side pass from which it exits back into the front-end head, and finally out of the heat exchanger from the tube fluid outlet (9). The shell-side fluid enters the heat exchanger from the shell inlet (2), flows on the shell side in a cross-parallel flow pattern in respect to the first pass, and cross-counter flow in respect to the tube pass, guided by baffle plates (8), and eventually exits from shell outlet (7). The tube bundle is held in place by the tube sheets (5), and inside the shell supported by the baffle plates [6].

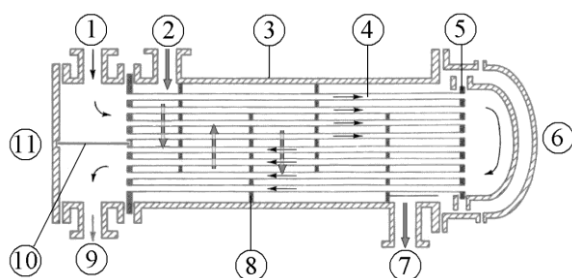


Fig 1. A shell and tube heat exchanger type 1-2.
Source: [6]

Condensers are used extensively in chemical and petroleum processing for distillation, refrigeration, and power generation systems. Condensers are an integral part of almost all the operations in the process industry. Condensers are basically two-phase flow heat exchangers in

which the heat is generated when vapours are converted to liquid. The heat generated is rejected to a cooling medium, which acts as a heat sink. In condensers, the latent heat is given up by the process fluid and transferred to the cooling medium. Cooling water or surrounding air is generally used as cooling medium in most of the operations in the industry. Usually, the vapors that enter a condenser are saturated, although in many operations, the process fluid may enter the condenser in the form of superheated vapors. This normally happens when the vapors are not obtained as distillate of a distillation column. The superheated vapors are first desuperheated until saturation and then condensation takes place. The process fluid then leaves the condenser as a saturated or a sub-cooled liquid, depending upon the temperature of the cooling medium and the condenser design [7].

Condensers can also be classified as partial or total. When a pure component is considered, it will condense isothermally and will be totally condensed. If a mixture of components is considered, then it can be either be condensed totally or partially based on process conditions [7]. Condensers can be horizontally or vertically oriented with the condensation on the tube-side or the shell-side. The magnitude of the condensing film coefficient for a given quantity of vapor condensation on a given surface is notably different depending on the orientation of the condenser. The condensation normally takes place on the shell-side of horizontal exchangers and the tube-side of vertical exchangers. Horizontal shell-side condensation is normally chosen because condensing film transfer coefficients are usually higher [8].

Shell and tube condensers are the most commonly used heat exchangers in process industries because of their relatively simple manufacturing and their adaptability to different operating conditions. Although this condenser type differentiates itself by low-pressure drops with high flow velocities, its capital requirement, as well as the combined power and capital cost requirement due to pressure drops of the pumped and compressed streams in a unit, can be very expensive [9].

Shell-and-tube condensers with condensation on the shell-side are widely used in both process and refrigeration industries. This usually means that the condensing medium is fed to the top of a shell-and-tube heat exchanger, and then while flowing on the outside of the tubes it condenses, leaving its latent heat to the cooling medium flowing inside the tubes. The condensed liquid is collected at the bottom of the shell where it leaves the condenser. The heat transfer in a shell-and-tube condenser is difficult to predict. Factors such as the complex geometry of the tube bank, effect of the tube surface geometry, vapour shear effects and condensate inundation from the tubes above all have an effect on heat transfer [10].



In a broad sense, the design of a new heat exchanger means the determination/selection of an exchanger construction type, flow arrangement, tube material, and the physical size of an exchanger to meet the specified heat transfer and pressure drops within all specified constraints. For a STHE a sizing problem generally refers to the determination of shell type, diameter and length; number of tubes; tube layout; pass arrangement; heat exchange area; overall heat transfer coefficient; pressure drop, fluids velocities and Reynolds number of both fluids; as well as many other parameters. Inputs to the sizing problem are fluid flow rates, inlet and outlet fluid temperatures, fouling factors; diameters, length and material of tubes, and maximum possible pressure drop of the two fluids involved [2].

There are several studies reported where a shell and tube condenser is designed, sized or studied for a particular heat exchange service. In this sense, in [11] a shell and tube heat exchanger was designed to condense 0.03 kg/s of a superheated steam stream from 320 °C (2 bar) to 120 °C, using water as coolant. Also, [7] designed a shell and tube desuperheater-condenser for ammonia-water system by using standard correlations based on Kern's method, while the results were compared with HTRI Xchanger Suite Educational 6.0 software. Likewise, [2] carried out the geometry optimization of a shell and tube heat exchanger working as a condenser in a brewing company, where 6,000 kg/h of steam enters at 160 °C on the shell side to heat cooled water to an outlet temperature of 35.5 °C. Several parameters were calculated such as heat load, pressure drop, optimum insulation cost, tube length, thickness and tube patterns, among others, thus selecting the allowable design from the thermal design point of view. In [12] a conceptual technological design aspect of a super vacuum hybrid surface steam condenser was theoretically analyzed. Similarly, in [13] the redesign and construction of a shell and tube condenser intended for the study of forced convection, with and without changing phase, was developed with the purpose of providing a laboratory of an equipment to perform practical experiences that could be used to analyze such phenomena. In this study, the research was conducted in three phases: 1) diagnosis, carried out through survey techniques; 2) the techno-economic feasibility, which involved the redesign, material selection, and cost determination; and 3) construction and operational testing of the redesigned condenser. In [14] an optimization of a shell and tube condenser was performed for a low temperature thermal desalination plant. Also, in [15] a procedure was proposed for the design of the components of a heat exchanger network, including the condensers of the network, using pinch analysis to maximize heat recovery for a given minimum temperature difference, and using genetic algorithm in order to minimize its total annual cost. Other authors [9] studied the effect of baffle spacing on heat transfer area and pressure drop for shell side condensation in the most common types of segmentally baffled shell and tube condensers (TEMA E and J types with

conventional tube bundles), while a set of correlations were also presented to calculate the optimum baffle spacing. In [16] a shell and tube condenser was designed from both the thermal and mechanical points of view, for its application in a steam turbine of a thermal power plant. In [10] a detailed 2D Computational Fluid Dynamics (CFD) calculation for vapour flow field and condensation rate was carried out for geometry similar to a real full-scale shell-and-tube condenser with 100 tubes, with condensation occurring on the shell-side. The differences in vapour flow behaviour were investigated for pure R22 and for a binary mixture of R32 and R134a. In [17] a dynamic mathematical model of a shell-and-tube condenser operating in a vapour compression refrigeration plant was presented and validated. The model was formulated from mass continuity, energy conservation and heat transfer physical fundamentals by using a lumped-parameter formulation for the condenser that is similar to the ones presented in previous studies, but with some differences in the selection of control volumes and including the refrigerant dynamics in a simplified way. In [18] a thermo-economic optimization of a shell and tube condenser was presented, based on two new optimization methods, namely genetic and particle swarm (PS) algorithms. The procedure was selected to find the optimal total cost including investment and operation cost of the condenser. Initial cost included condenser surface area and operational cost involved pump output power to overcome the pressure loss. In [19] a moving-boundary lumped parameter (MB) dynamic model of a shell-and-tube condenser was proposed, where the mean void fraction (MVF) correlation used can be changed in order to analyze the influence of the MVF correlation on the model performance, comparing the predictions obtained with experimental data using MVF correlations frequently mentioned in the literature. The experimental data used consisted of transients obtained varying the working conditions in a wide range, and being the MVF correlations used derived from different local void fraction expressions which allowed a relatively easy analytical or numerical integration. In [20] the energy, exergy and economic assessments of a shell and tube condenser of 580 MW nuclear power plant was carried out using different water-based hybrid nanofluids as coolant. The effect of nanoparticle concentration on reductions of coolant requirement, pumping power and operating cost was also investigated. Similarly, in [21] the constructal design of a shell-and-tube condenser with ammonia-water as the working fluid was studied based on constructal theory. A complex function (CF) formed by entropy generation rate (EGR) and total pumping power (TPP) was minimized, and the tube diameter was optimized, while the parameter that influences on the optimal results were researched. In [22] a horizontal shell and tube condenser was designed from the thermo-hydraulic point of view using the calculation approach reported by [23], in order to condense ethanol vapours using chilled water as coolant. Finally, in [24] a linear design optimization approach was presented for the

first time for horizontal shell and tube condensers that guarantees global optimality. The numerical results obtained in this study indicated that the proposed approach can present solutions with lower heat transfer areas than two design procedures presented in chemical process design textbooks.

There are textbooks [8,25,26,27] that present several design methodologies related with the design of condensers using heuristics based on choices made by the designer. The main concept is to find one viable exchanger, not necessarily the optimal one [24].

In certain chemical processing plant, a vapour stream of pure methanol is obtained at the overhead of a distillation column, and it is desired to condense it using a shell and tube heat exchanger. In this context, in the present paper a 1-2 shell and tube condenser was designed from the thermo-hydraulic point of view, in order to condense methanol vapours by using chilled water as coolant. To accomplish this task, the calculation approach described in [23] was applied, where several important design parameters were calculated such as the number of tubes, heat exchange area, shell internal diameter, overall heat transfer coefficient and the pressure drops of both fluids.

2. Materials y methods.

2.1. Problem statement.

It's desired to condense 30,000 kg/h of methanol vapours that comes from the overhead of a distillation column at a temperature of 120 °C. Chilled water is available at 2 °C for this service, while the temperature rise is to be limited to 13 °C for this coolant. According to plant standards, stainless steel tubes with a nominal diameter of ¾ inch 40ST are required, with a length of 5.0 m. The condenser is to operate at 5.0 bar, the vapours are to be totally condensed and no subcooling is required. The pressure drop of the chilled water and methanol should not exceed 100,000 Pa and 10,000 Pa, respectively. Design a suitable horizontal one shell, two tube pass (1-2) shell and tube heat exchanger for this condensation service, using a flow arrangement of countercurrent type.

2.2. Calculation methodology.

2.2.1. Heat exchange area of the condenser.

The calculation steps included in the calculation procedure to design the horizontal shell and tube heat condenser are presented below, specifically to determine the heat exchange area.

Step 1. Definition of the initial parameters:

- Vapour flowrate (m_v): [kg/h].
- Operating pressure of the condenser (P_c): [bar].
- Inlet temperature of vapour (T_1): [°C].

- Condensation temperature of vapour at the operating pressure of condenser (T_c): [°C].
- Molecular weight of methanol (M_v): [kg/kmol].
- Enthalpy of vapour methanol at T_c and P_c (h_v): [kJ/kg].
- Enthalpy of liquid (condensate) methanol at T_c and P_c (h_L): [kJ/kg].
- Inlet temperature of chilled water (t_1): [°C].
- Outlet temperature of chilled water (t_2): [°C].
- Inside diameter of tubes (d_i): [m].
- Outside diameter of tubes (d_e): [m].
- Length of tubes (L_t): [m].
- Thermal conductivity of the tubes material (k_w): [W/m.K].
- Fouling factor of water (R_w): [K.m²/W].
- Fouling factor of condensing methanol (R_m): [K.m²/W].
- Number of tube side passes (n_t).

Step 2. Heat duty (Q):

$$Q = \frac{m_v}{3,000} \cdot (h_v - h_L) \quad (1)$$

Step 3. Assumption of the overall heat transfer coefficient (U_a).

Step 4. Location of fluids inside the shell and tube heat exchanger.

The vapours will be located in the shell side, while the chilled water will flow inside the tubes.

Step 5. Log mean temperature difference ($LMTD$):

$$LMTD = \frac{(T_1 - t_2) - (T_c - t_1)}{\ln \frac{(T_1 - t_2)}{(T_c - t_1)}} \quad (2)$$

Step 6. Factor R:

$$R = \frac{T_1 - T_c}{t_2 - t_1} \quad (3)$$

Step 7. Factor S:

$$S = \frac{t_2 - t_1}{T_1 - t_1} \quad (4)$$

Step 8. Temperature correction factor (F_t):

For a 1 shell: 2 tube pass heat exchanger, the correction factor is given by the following equation:

$$F_t = \frac{\sqrt{(R^2 + 1)} \cdot \ln \left[\frac{(1 - S)}{(1 - R \cdot S)} \right]}{(R - 1) \cdot \ln \left[\frac{2 - S \left[R + 1 - \sqrt{(R^2 + 1)} \right]}{2 - S \left[R + 1 + \sqrt{(R^2 + 1)} \right]} \right]} \quad (5)$$

Step 9. True temperature difference (ΔT_m):

$$\Delta T_m = LMTD \cdot F_t \quad (6)$$

Step 10. Trial heat exchange area (A_o):

$$A_o = \frac{Q \cdot 1,000}{U_a \cdot \Delta T_m} \quad (7)$$

Step 11. Surface area of one tube (a_t):

Ignoring the tube sheet thickness [23]:

$$a_t = \pi \cdot d_e \cdot L_t \quad (8)$$

Where d_e and L_t are given in m.

Step 12. Number of tubes (N_T):

$$N_T = \frac{A_o}{a_t} \quad (9)$$

Step 13. Tube pitch (p_t):

A square pitch is selected. Thus:

$$p_t = 1.25 \cdot d_e \quad (10)$$

Where d_e is given in mm.

Step 14. Tube bundle diameter (D_b):

$$D_b = d_e \cdot \left(\frac{N_T}{K_1} \right)^{1/n_1} \quad (11)$$

Where d_e is given in mm, while K_1 and n_1 are constants that depend on the type of pitch selected and the number of tube passes [23].

Step 15. Number of tubes in centre row (N_r):

$$N_r = \frac{D_b}{p_t} \quad (12)$$

Where both D_b and p_t are given in mm.

Step 16. Assume a condensation film coefficient ($h_{c(a)}$).

Step 17. Mean temperature of both the shell-side (\bar{T}) and tube-side (\bar{t}) fluids:

- Shell side (methanol vapours):

$$\bar{T} = \frac{T_1 + T_c}{2} \quad (13)$$

- Tube side (chilled water):

$$\bar{t} = \frac{t_1 + t_2}{2} \quad (14)$$

Step 18. Tube wall temperature (T_w):

$$T_w = \bar{T} - \frac{(\bar{T} - \bar{t}) \cdot U_a}{h_{c(a)}} \quad (15)$$

Step 19. Mean temperature condensate (T_w):

$$\bar{T}_C = \frac{\bar{T} + T_w}{2} \quad (16)$$

Step 20. Physical properties of the liquid methanol at the mean temperature condensate (T_w):

- Viscosity (μ_L) [Pa.s].
- Density (ρ_L) [kg/m³].
- Thermal conductivity (k_L) [W/m.K].

Step 21. Density of vapour methanol at mean vapour temperature (ρ_v):

$$\rho_v = \frac{M_v}{22.4} \cdot \frac{273}{273 + \bar{T}} \cdot \frac{P_c}{P_o} \quad (17)$$

Where P_o is 1.0 bar.

Step 22. Condensate loading on a horizontal tube (Γ_h):

$$\Gamma_h = \frac{\dot{m}_v}{3,600 \cdot L_t \cdot N_T} \quad (18)$$

Step 23. Average number of tubes in a vertical tube row (N_{tr}):

$$N_{tr} = \frac{2}{3} \cdot N_r \quad (19)$$

Step 24. Calculated mean condensation film coefficient for a tube bundle ($h_{c(b)}$):

$$h_{c(b)} = 0.95 \cdot k_L \cdot \left[\frac{\rho_L \cdot (\rho_L - \rho_v) \cdot g}{\mu_L \cdot \Gamma_h} \right]^{1/3} \cdot N_{tr}^{-1/6} \quad (20)$$

Where g is the gravitational acceleration = 9.81 m/s².

Step 25. Verification of the mean condensation film coefficient calculated in step 24 [$h_{c(b)}$] with the mean condensation coefficient assumed in step 16 [$h_{c(a)}$].

In this approach, if the value of $h_{c(b)}$ is close enough to the assumed value [$h_{c(a)}$] then no correction of T_w is necessary.

Step 25. Tube cross-sectional area (a_{ct}):

$$a_{ct} = \frac{\pi}{4} \cdot d_i^2 \cdot \frac{N_T}{n_t} \quad (21)$$

Where d_i is given in m.

Step 26. Density of tube-side fluid (chilled water) at \bar{t} (ρ_t).

Step 27. Heat capacity of the tube-side fluid (chilled water) at \bar{t} (Cp_t).

Step 28. Required flowrate of the tube-side fluid (chilled water) (m_t):

$$m_t = \frac{Q}{(t_2 - t_1) \cdot Cp_t} \quad (22)$$

Where Q is given in kW.

Step 29. Velocity of the tube-side fluid (u_t):

$$u_t = \frac{m_t}{\rho_t \cdot a_{ct}} \quad (23)$$

Step 30. Film coefficient for the tube side fluid (h_t):

- Specifically for water:

$$h_t = \frac{4,200 \cdot (1.35 + 0.02 \cdot \bar{t}) \cdot u_t^{0.8}}{d_i^{0.2}} \quad (24)$$

Where d_i is given in mm.

Step 31. Overall heat transfer coefficient calculated (U_c):

$$U_c = \frac{1}{\frac{1}{h_{c(b)}} + R_m + \frac{d_e \cdot \ln\left(\frac{d_e}{d_i}\right)}{2 \cdot k_w} + \frac{d_e}{d_i} \cdot R_w + \frac{d_e}{d_i} \cdot \frac{1}{h_t}} \quad (24)$$

Where d_e and d_i are given in m.

Step 32. Compare the calculated overall heat transfer coefficient (U_c) with the overall heat transfer coefficient assumed in step 3 (U_a).

If the values are significantly different, then the calculation procedure should be repeated using a new trial assumed value for U_a which could be close enough to U_c .

2.3. Pressure drops.

2.3.1. Shell side pressure drop.

Step 33. Selection of the heat exchanger.

Step 34. Selection of the baffle spacing (l_B) and cut.

Step 35. Clearance (C_t).

Step 36. Shell internal diameter (D_s):

$$D_s = D_b + C_t \quad (25)$$

Where both D_b and C_t are given in mm.

Step 37. Cross-flow area (A_s):

$$A_s = \frac{(p_t - d_e)}{p_t} \cdot D_s \cdot l_B \quad (26)$$

Where all the parameters are given in m.

Step 38. Mass velocity of the vapour (G_v):

$$G_v = \frac{m_v}{3,600 \cdot A_s} \quad (27)$$

Step 39. Viscosity of the methanol vapour (μ_v) at the mean temperature \bar{T} .

Step 40. Linear velocity of the vapour (u_v):

$$u_v = \frac{G_v}{\rho_v} \quad (28)$$

Step 41. Shell-side equivalent diameter (D_{eq}):

- For square pitch arrangement:

$$D_{eq} = \frac{1.27}{d_e} \cdot (p_t^2 - 0.785 \cdot d_e^2) \quad (29)$$

Where both d_e and p_t are given in m.

Step 42. Reynolds number of the vapour (Re_v):

$$Re_v = \frac{G_v \cdot D_{eq}}{\mu_v} \quad (30)$$

Step 43. Shell-side friction factor (j_s)

Step 44. Pressure drop of the shell-side fluid (vapour) (ΔP_v):

The pressure drop of the shell side fluid can be assumed as 50% of that calculated using the inlet flow. Thus:

$$\Delta P_v = \frac{1}{2} \cdot \left[8 \cdot j_s \cdot \left(\frac{D_s}{D_{eq}} \right) \cdot \left(\frac{L_t}{l_B} \right) \cdot \frac{\rho_v \cdot (u_v)^2}{2} \cdot \left(\frac{\mu_v}{\mu_w} \right)^{-0.14} \right] \quad (31)$$

Where D_s and d_e are given in mm, while L_t and l_B are given in m. The term $(\mu_v/\mu_w)^{-0.14}$, which is the viscosity correction factor, could be neglected [23].

2.3.2. Tube side pressure drop.

Step 45. Viscosity of tube-side fluid (chilled water) at \bar{t} (μ_t).

Step 46. Reynolds number of tube-side fluid (chilled water) (Re_t):

$$Re_t = \frac{u_t \cdot \rho_t \cdot d_i}{\mu_t} \quad (32)$$

Where d_i is given in m.

Step 47. Tube-side friction factor (j_t).

Step 48. Pressure drop of the tube-side fluid (chilled water) (ΔP_t):

$$\Delta P_t = n_t \cdot \left[8 \cdot j_t \cdot \left(\frac{L_t}{d_i} \right) \cdot \left(\frac{\mu_t}{\mu_w} \right)^{-0.14} + 2.5 \right] \cdot \frac{\rho_t \cdot u_t^2}{2} \quad (33)$$

Where the term $(\mu_t/\mu_w)^{-0.14}$ can be neglected [23] and L_t and d_i are given in m.

3. Results

3.1. Heat exchange area of the condenser

Step 1. Definition of the initial parameters

Table 1 shows the initial parameters required to design the horizontal shell and tube condenser.

Table 1. Initial parameters required to design the horizontal shell and tube condenser.

Parameter	Symbol	Value	Unit
Vapour flowrate	m_v	30,000	kg/h
Operating pressure of the condenser	P_c	5.0	bar
Inlet temperature of vapour	T_1	120	°C
Condensation temperature of vapour at the operating pressure of condenser ¹	T_c	110.73	°C
Molecular weight of methanol ¹	M_v	32.04	kg/kmol
Enthalpy of vapour methanol at T_c and P_c ¹	h_v	1,134.12	kJ/kg
Enthalpy of liquid methanol at T_c and P_c ¹	h_L	141.42	kJ/kg
Inlet temperature of chilled water	t_1	2	°C



Outlet temperature of chilled water	t_2	15	°C
Inside diameter of tubes ¹	d_i	20.93	m
Outside diameter of tubes ¹	d_e	26.67	m
Length of tubes	L_t	5.0	m
Thermal conductivity of the tubes material ²	k_w	16	W/m.K
Fouling factor of water ²	R_w	0.00035	K.m ² /W
Fouling factor of condensing methanol ²	R_m	0.00020	K.m ² /W
Number of tube side passes	n_t	2	

¹As reported by [28].

²As reported by [23].

Source: Own elaboration.

Table 2 presents the results of the parameters calculated in steps 2-15.

Table 2. Results of the parameters calculated in steps 2-15.

Step	Parameter	Symbol	Value	Units
2	Heat duty	Q	8,272.5	kW
3	Assumption of the overall heat transfer coefficient ¹	U_a	650	W/m ² .K
5	Log mean temperature difference ²	$LMTD$	106.87	°C
6	Factor R	R	0.713	-
7	Factor S	S	0.110	-
8	Temperature correction factor	F_t	0.998	
9	True temperature difference	ΔT_m	106.65	°C
10	Trial heat exchange area	A_o	119.33	m ²
11	Surface area of one tube	a_t	0.419	m ²
12	Number of tubes	N_T	~ 285	-
13	Tube pitch	p_t	33.34	mm
14	Tube bundle diameter ³	D_b	707.56	mm
15	Number of tubes in centre row	N_r	~ 22	-

¹As reported by [26] in the range of 550-1,100 W/m².K for the condensation of organic solvents in shell and tube, water-cooled condensers.

²The condensation range is small and the change in saturation temperature will be linear, so the log mean temperature difference can be used [23].

³The constants K_1 and n_1 have values of 0.156 and 2.291 respectively, for a square pitch and two tube passes [23].

Source: Own elaboration.

Step 16. Assume a condensation film coefficient ($h_{c(a)}$).

According to the range reported by [8] of 1,000-2,500 W/m².K for the condensation of low viscosity organic compounds, a value of 1,600 W/m².K was assumed for the condensation film coefficient of methanol on the shell side.

Table 3 displays the results of the parameters calculated in steps 17-24.

Table 3. Results of the parameters calculated in steps 17-24.

Step	Parameter	Symbol	Value	Units
17	Mean temperature of methanol	\bar{T}	115.36	°C
	Mean temperature of chilled water	\bar{t}	8.50	°C
18	Tube wall temperature	T_w	71.95	°C
19	Mean temperature condensate	T_w	93.66	°C
20	Viscosity of liquid methanol ¹	μ_L	0.000269	Pa.s
	Density of liquid methanol ¹	ρ_L	717.38	kg/m ³
	Thermal conductivity of liquid methanol ¹	k_L	0.1806	W/m.K
21	Density of vapour methanol at \bar{T}	ρ_v	5.027	kg/m ³
22	Condensate loading on a horizontal tube	Γ_h	0.0058	kg/s.m
23	Average number of tubes in a vertical tube row	N_{tr}	~ 15	-
24	Calculated mean condensation film coefficient for a tube bundle	$h_{c(b)}$	1,611.97	W/m ² .K

¹As reported by [28].

Source: Own elaboration.

Step 25. Verification of the mean condensation film coefficient calculated in step 24 [$h_{c(b)}$] with the mean condensation coefficient assumed in step 16 [$h_{c(a)}$].

Since the calculated mean condensation film coefficient ($h_{c(b)} = 1,611.97$ W/m².K) is close enough to the assumed

value in step 16 ($h_{c(a)} = 1,600 \text{ W/m}^2.\text{K}$), then no correction of the tube wall temperature (T_w) is needed.

Table 4 describes the results of the parameters calculated in steps 25-31.

Table 4. Results of the parameters calculated in steps 25-31.

Step	Parameter	Symbol	Value	Units
25	Tube cross-sectional area	a_{ct}	0.049	m^2
26	Density of chilled water at \bar{t}	ρ_t	999.818	kg/m^3
27	Heat capacity of chilled water at \bar{t}	Cp_t	4.1977	kJ/kg.K
28	Required flowrate of chilled water	m_t	151.59	kg/s
29	Velocity of chilled water	u_t	3.094	m/s
30	Film coefficient for chilled water	h_t	8,576.87	$\text{W/m}^2.\text{K}$
31	Calculated overall heat transfer coefficient	U_c	618.47	$\text{W/m}^2.\text{K}$

Source: Own elaboration.

Step 32. Comparison of the calculated overall heat transfer coefficient (U_c) with the overall heat transfer coefficient assumed in step 3 (U_a):

The value of the overall heat transfer coefficient calculated in step 31 ($U_c = 618.47 \text{ W/m}^2.\text{K}$) is close enough to the overall heat transfer coefficient assumed in step 3 ($U_a = 650 \text{ W/m}^2.\text{K}$), so there is no need to repeat the calculation procedure and carry out a new trial, and the heat exchanger area of the condenser will be 119.33 m^2 .

3.2. Pressure drops.

3.2.1. Shell side pressure drop

Step 33. Selection of the heat exchanger.

In this study we select a pull-through floating head heat exchanger, with no need for close clearance. The reported advantages of these heat exchangers include that they are more versatile than fixed head and U-tube exchangers, are suitable for high temperature differentials and, as the tubes can be rodded from end to end and the bundle removed, are easier to clean and can be used for fouling liquids [23].

Step 34. Selection of the baffle spacing (l_B) and cut.

As specified by [23], the baffle spacings used in commercial shell and tube heat exchangers range from 0.2 to 1.0 shell internal diameter (D_s). Close baffle spacing will give higher heat-transfer coefficients, but at the expense of higher pressure drops. The optimum spacing will usually be

between 0.3 to 0.5 times the shell diameter. However, although the construction of a condenser is similar to other shell and tube exchangers, wider baffle spacings are applied, typically $l_B = D_s$ [23]. In this study we obeyed this last rule-of-thumb, that is, we selected a value for the baffle spacing equal to the shell internal diameter.

The term “baffle cut” is used to specify the dimensions of a segmental baffle. The baffle cut is the height of the segment removed to form the baffle, expressed as a percentage of the baffle disc diameter. Baffle cuts from 15 to 45 % are commonly used [23]. In this study, we chose a baffle cut of 45%.

Step 35. Clearance (C_t).

According to [23], for a value of the tube bundle diameter (D_b) of 707.56 mm (0.707 m), the clearance will be 93 mm for a pull-through floating head heat exchanger.

Step 36. Shell internal diameter (D_s):

$$D_s = D_b + C_t = 707.56 + 93 = 800.56 \text{ mm} \quad (25)$$

Thus, the baffle spacing (l_B) will be 800.56 mm.

Table 5 exhibits the results of the parameters calculated in steps 37-44.

Table 5. Results of the parameters calculated in steps 37-44.

Step	Parameter	Symbol	Value	Units
37	Cross-flow area	A_s	0.128	m^2
38	Mass velocity of the vapour	G_v	65.10	$\text{kg/m}^2.\text{s}$
39	Viscosity of the methanol vapour at the mean temperature \bar{T}	μ_v	0.0000128	Pa.s
40	Linear velocity of the vapour	u_v	12.95	m/s
41	Shell-side equivalent diameter	D_{eq}	0.0263	m
42	Reynolds number of the vapour	Re_v	133,760.15	-
43	Shell-side friction factor ¹	f_s	0.023	-
44	Pressure drop of methanol (vapour)	ΔP_v	7,372.55	Pa

¹For a baffle cut of 45% and a Reynolds number of 1.34×10^5 [23].

Source: Own elaboration.

3.2.2. Tube side pressure drop.

Table 6 shows the results of the parameters calculated in steps 45-48.

Table 6. Results of the parameters calculated in steps 45-48.

Step	Parameter	Symbol	Value	Units
45	Viscosity of chilled water at \bar{t}	μ_t	0.001364	Pa.s
46	Reynolds number of chilled water	Re_t	47,467.47	-
47	Tube-side friction factor	f_t	0.0033	-
48	Pressure drop of the chilled water ¹	ΔP_t	84,289.69	Pa

¹For a Reynolds number of $4,74 \times 10^4$ [23].

Source: Own elaboration.

4. Discussion.

The heat duty for this heat exchange service was 8,272.5 kW, with a true temperature difference of 106.65 °C. In [7] a shell and tube desuperheater-condenser was designed to condense a stream of ammonia using cooling water as coolant, and by using the standard correlations based on Kern's method. In this study, the calculated heat duty is 903.78 kW. In [23] the heat duty is 4,368.8 kW for a horizontal shell and tube condenser designed to condense a stream of mixed light hydrocarbon vapours using cooling water. In [8] a horizontal shell and tube condenser is designed to condense acetone vapours on the shell side by using cooling water as coolant, thus obtaining a calculated heat duty of 2,865 kW. In another study [22], a value for the calculated heat duty of 6,578.47 kW was obtained for a horizontal shell and tube condenser designed to condense a stream of ethanol vapours.

The calculated film coefficient for chilled water (8,576.87 W/m².K) was 5.32 times higher than the calculated mean condensation film coefficient for the condensing methanol vapours (1,611.97 W/m².K). This result doesn't agree with the findings of [7], where the mean condensation film coefficient of an ammonia stream condensing on the shell side (11,836.73 W/m².K) is 1.80 times higher than the heat transfer coefficient of the cooling water on the tube side (6567.32 W/m².K). It's worth mentioning that in this study [7] the horizontal shell and tube heat exchanger was also designed using the HTRI software, and the results obtained by this software regarding the calculation of the film heat transfer coefficients for both streams agree with those reported on the present study, that is, the value of the film heat transfer coefficient for cooling water (7,081.82 W/m².K) is higher (1.41 times) than the mean condensation film coefficient of condensing ammonia on the shell side (4,995.21 W/m².K). In [23] the calculated film coefficient for cooling water flowing inside the tubes (7,097 W/m².K) is 4.90 times higher than the calculated mean condensation film coefficient (1,447 W/m².K) for the mixed light hydrocarbon stream condensing on the shell side. In [8], the calculated film coefficient for a cooling water stream

flowing on the tube side (7,483 W/m².K) is 5.02 times higher than the calculated mean condensation film coefficient (1,491 W/m².K) for the acetone stream condensing on the shell side. In [22] the value of tube side heat transfer coefficient for chilled water is 6,265.59 W/m².K, which is 7.55 times higher than the mean condensation film coefficient for the ethanol condensing vapours (829.38 W/m².K). The value of the film coefficient for chilled water calculated in this study is higher than the range suggested by [8] of 2,000-6,000 W/m².K, while the value of the mean condensation film coefficient for the condensing methanol vapours agrees with the range reported by the same author of 1,000–2,500 W/m².K.

Respecting the overall heat transfer coefficient calculated in this study (618.47 W/m².K), its value agrees with the range reported by [26] of 550-1,100 W/m².K; the range reported by [25] of 300-1,000 W/m².K, and the range reported by [28] of 568-1,136 W/m².K, while it's slightly lower than the range reported by [23] of 700-1,000 W/m².K.

About 151.59 kg/s of chilled water will be needed in this study to carry out the condensation of the pure methanol vapours. In [8], a flowrate of cooling water of 68.54 kg/s is needed to condense 5.8 kg/s of acetone vapours. In [23] a flowrate of cooling water of 104.5 kg/s is needed to condense 12.5 kg/s of mixed light hydrocarbon vapours. In [22] about 157 kg/s are needed to condense 6.94 kg/s of pure ethanol vapours. In [7] the flowrate of cooling water required to condense 0.6841 kg/s of ammonia vapours is 35.97 kg/s.

The shell and tube condenser designed in this paper will have the following parameters:

- Heat exchange area: 119.33 m².
- Number of tubes: 285.
- Tube bundle diameter: 707.56 mm.
- Number of tubes in centre row: 22.
- Shell internal diameter: 800.56 mm.

In [7], the horizontal desuperheater-condenser designed to carry out the condensation of ammonia vapours, has the following design parameters:

- Heat exchange area: 116.62 m².
- Number of tubes: 784.
- Shell internal diameter: 840 mm.

In [8], the horizontal shell and tube condenser designed to condense acetone vapours using cooling water, has the following design results:

- Heat exchange area: 96.0 m².
- Number of tubes: 488.
- Shell internal diameter: 623 mm.

In [23] the horizontal shell and tube heat exchanger condenser designed to condense a stream of mixed light hydrocarbon vapours has the following design parameters:



- Heat exchange area: 364 m².
- Number of tubes: 1194.
- Shell internal diameter: 1130 mm.

In [22] the horizontal shell and tube heat exchanger condenser designer to condense a stream of ethanol vapours has the design parameters presented below:

- Heat exchange area: 223.68 m².
- Number of tubes: 731.
- Tube bundle diameter: 744.57 mm.
- Shell internal diameter: 1,684 mm.

The calculated pressure drop for the chilled water was 84,289.69 Pa, which is 11.43 times higher than the calculated pressure drop of the condensing methanol (7,372.55 Pa). Both values of the pressure drop are below the limits established by the heat transfer process. In [23] the pressure drop of the cooling water flowing inside the tubes (53,000 Pa) is 40.77 times higher than the pressure drop of a mixed light hydrocarbon vapours condensing on the shell side (1,300 Pa). Likewise, in [7] the pressure drop of cooling water flowing inside the tubes (49,130 Pa) is 40.16 times higher than the pressure drop of condensing ammonia on the shell (1,223.4 Pa). In [22], the pressure drop of the chilled water stream located in the tubes (42,192.63 Pa) is 4.19 times higher than the pressure drop of the condensing ethanol on the shell side (10,069.25 Pa).

5. Conclusions.

In the present work a 1-2 horizontal shell and tube condenser was designed from the thermo-hydraulic point of view to condense a stream of pure methanol vapours using chilled water as coolant. The design calculation methodology employed to carry out the design task was the reported in [23]. Several key design parameters were calculated such as the heat transfer area (119.33 m²); the number of tubes (285); the tube bundle diameter (707.56 mm) and the shell internal diameter (800.56 mm). Other important thermal parameters were also computed such as the heat duty (8,272.5 kW), the overall heat transfer coefficient (618.47 W/m².K) and the required flowrate of chilled water (151.59 kg/s). The calculated values of the pressure drop of both the shell-side (7,372.55 Pa) and tube-side (84,289.69 Pa) fluids were below the maximum limit set by the heat exchanger process. The designed 1-2 shell and tube condenser is of pull-through floating head type, with a tube length of 5.0 m, a baffle cut of 45% and a baffle spacing of 800.56 mm.

6.- Author Contributions.

1. Conceptualization: Amaury Pérez Sánchez.
2. Data curation: Heily Victoria González, Elizabeth Ranero González.
3. Formal analysis: Amaury Pérez Sánchez, Arlenis Cristina Alfaro Martínez, Eddy Javier Pérez Sánchez.
4. Acquisition of funds: Not applicable.

5. Research: Amaury Pérez Sánchez, Heily Victoria González, Eddy Javier Pérez Sánchez.
6. Methodology: Amaury Pérez Sánchez, Arlenis Cristina Alfaro Martínez, Elizabeth Ranero González.
7. Project management: Not applicable.
8. Resources: Not applicable.
9. Software: Not applicable.
10. Supervision: Amaury Pérez Sánchez.
11. Validation: Amaury Pérez Sánchez.
12. Writing - original draft: Eddy Javier Pérez Sánchez, Elizabeth Ranero González.
13. Writing - revision and editing: Amaury Pérez Sánchez, Heily Victoria González.

7.- References

- [1] E. J. Fernandes and S. H. Krishnamurthy, "Design and analysis of shell and tube heat exchanger," *Int. J. Simul. Multidisci. Des. Optim.*, vol. 13, no. 15, pp. 1-8, 2022. <https://doi.org/10.1051/smdo/2022005>
- [2] D. Bogale, "Design and Development of Shell and Tube Heat Exchanger for Harar Brewery Company Pasteurizer Application (Mechanical and Thermal Design)," *American Journal of Engineering Research*, vol. 03, no. 10, pp. 99-109, 2014.
- [3] P. Bichkar, O. Dandgaval, P. Dalvi, R. Godase, and T. Dey, "Study of Shell and Tube Heat Exchanger with the Effect of Types of Baffles," *Procedia Manufacturing*, vol. 20, pp. 195-200, 2018. <https://doi.org/10.1016/j.promfg.2018.02.028>
- [4] B. M. Reyes, "Diseño de un intercambiador de calor (condensador) para el sistema de la Bomba de Vapor Desalinizadora Solar de Alta Potencia del proyecto Walfisch," Tesis de Diploma, Universidad Técnica Federico Santa María, Valparaíso, Chile, 2021.
- [5] I. C. Nwokedi and C. A. Igwegbe, "Design of Shell and Tube Heat Exchanger with Double Passes," *Journal of Engineering Research and Reports*, vol. 3, no. 4, pp. 1-12, 2018. <https://doi.org/10.9734/JERR/2018/v3i416883>
- [6] J. Saari, *Heat Exchanger Dimensioning*. Lappeenranta, Finland: Lappeenranta University of Technology, 2015.
- [7] S. Sahajpal and P. D. Shah, "Thermal Design of Ammonia Desuperheater-Condenser and Comparative Study with HTRI," *Procedia Engineering*, vol. 51, pp. 375-379, 2013. <https://doi.org/10.1016/j.proeng.2013.01.052>
- [8] R. Smith, *Chemical Process Design and Integration*. West Sussex, England: John Wiley & Sons Ltd., 2005.
- [9] B. K. Soltan, M. Saffar-Avval, and E. Damangir, "Minimizing capital and operating costs of shell and tube condensers using optimum baffle spacing," *Applied Thermal Engineering*, vol. 24, pp. 2801-2810, 2004. <https://doi.org/10.1016/j.applthermaleng.2004.04.005>
- [10] T. Karlsson and L. Vamling, "Flow fields in shell-and-tube condensers: comparison of a pure refrigerant and a binary mixture," *International Journal of Refrigeration*, vol. 28, pp. 706-713, 2005. <https://doi.org/10.1016/j.jirefrig.2004.12.008>
- [11] D. E. Dana, "Diseño de un condensador para un loop experimental para probar maniobras de arranque del reactor CAREM," Proyecto Integrador, Universidad Nacional de Cuyo, Mendoza, Argentina, 2016.
- [12] R. K. Kapooria, S. Kumar, and K. S. Kasana, "Technological investigations and efficiency analysis of a steam heat exchange condenser: conceptual design of a hybrid steam condenser," *Journal of Energy in Southern Africa*, vol. 19, no. 3, pp. 35-45, 2008.
- [13] M. Lucena, C. Linárez, and E. Rodríguez, "Rediseño y construcción de un condensador para el estudio de convección forzada," *REDIP. UNEXPO. VRB. Venezuela*, vol. 5, no. 4, pp. 941-957, 2015.
- [14] R. Elakkiyadasan, P. M. Kumar, M. Subramanian, N. Balaji, M. Karthick, and S. Kaliappan, "Optimization of Shell and Tube Condenser for Low Temperature Thermal Desalination Plant," *E3S Web of Conferences*, vol. 309, p. 01011, 2021. <https://doi.org/10.1051/e3sconf/202130901011>



- [15] B. Allen, M. Savard-Goguen, and L. Gosselin, "Optimizing heat exchanger networks with genetic algorithms for designing each heat exchanger including condensers," *Applied Thermal Engineering*, vol. 29, pp. 3437–3444, 2009. <https://doi.org/10.1016/j.applthermaleng.2009.06.006>
- [16] J. Canoura, "Diseño de un condensador para planta de producción industrial," Trabajo de Fin de Grado, Universidad de La Coruña, La Coruña, España, 2016.
- [17] R. Llopis, R. Cabello, and E. Torrella, "A dynamic model of a shell-and-tube condenser operating in a vapour compression refrigeration plant," *International Journal of Thermal Sciences*, vol. 47, pp. 926–934, 2008. <https://doi.org/10.1016/j.ijthermalsci.2007.06.021>
- [18] H. Hajabdollahi, P. Ahmadi, and I. Dincer, "Thermoeconomic optimization of a shell and tube condenser using both genetic algorithm and particle swarm," *International Journal of Refrigeration*, vol. 34, pp. 1066–1076, 2011. <https://doi.org/10.1016/j.ijrefrig.2011.02.014>
- [19] V. Milián, J. Navarro-Esbrí, D. Ginestar, F. Molés, and B. Peris, "Dynamic model of a shell-and-tube condenser. Analysis of the mean void fraction correlation influence on the model performance," *Energy*, vol. 59, pp. 521–533, 2013. <http://dx.doi.org/10.1016/j.energy.2013.07.053>
- [20] S. K. Singh and J. Sarkar, "Energy, exergy and economic assessments of shell and tube condenser using hybrid nanofluid as coolant," *International Communications in Heat and Mass Transfer*, vol. 98, pp. 41–48, 2018. <https://doi.org/10.1016/j.icheatmasstransfer.2018.08.005>
- [21] H. Feng, C. Cai, L. Chen, Z. Wu, and G. Lorenzini, "Constructal design of a shell-and-tube condenser with ammonia-water working fluid," *International Communications in Heat and Mass Transfer*, vol. 118, p. 104867, 2020. <https://doi.org/10.1016/j.icheatmasstransfer.2020.104867>
- [22] A. Pérez, M. I. L. Rosa, Z. M. Sarduy, E. Ranero, and E. J. Pérez, "Thermo-hydraulic design of a horizontal shell and tube heat exchanger for ethanol condensation," *Nexo Revista Científica*, vol. 36, no. 04, pp. 551–571, 2023. <https://doi.org/10.5377/nexo.v36i04.16770>
- [23] R. Sinnott and G. Towler, *Chemical Engineering Design*, 6th ed. (Coulson and Richardson's Chemical Engineering Series). Oxford, United Kingdom: Butterworth-Heinemann, 2020.
- [24] I. P. S. Pereira, M. J. Bagajewicz, and A. L. H. Costa, "Global optimization of the design of horizontal shell and tube condensers," *Chemical Engineering Science*, vol. 236, p. 116474, 2021. <https://doi.org/10.1016/j.ces.2021.116474>
- [25] S. Kakaç, H. Liu, and A. Pramuanjaroenkij, *Heat Exchangers - Selection, Rating and Thermal Design*, 3rd ed. Boca Raton, U.S.A.: CRC Press, 2012.
- [26] E. Cao, *Heat transfer in process engineering*. New York, U.S.A.: The McGraw-Hill Companies, Inc., 2010.
- [27] M. Nitsche and R. O. Gbadamosi, *Heat Exchanger Design Guide - A Practical Guide for Planning, Selecting and Designing of Shell and Tube Exchangers*. Oxford, U.K.: Butterworth Heinemann, 2016.
- [28] D. W. Green and M. Z. Southard, *Perry's Chemical Engineers' Handbook*, 9th ed. New York, U.S.A.: McGraw-Hill Education, 2019.

Nomenclature

a_{ct}	Tube cross-sectional area	m ²
a_t	Surface area of one tube	m ²
A_o	Heat exchange area	m ²
A_s	Cross-flow area	m ²
C_p	Heat capacity	kJ/kg.K
C_t	Clearance	mm
d_i	Inside diameter of tubes	m
d_e	Outside diameter of tubes	m
D_b	Tube bundle diameter	mm
D_{eq}	Shell-side equivalent diameter	m
D_s	Shell internal diameter	mm

F_t	Temperature correction factor	-
g	Gravitational acceleration	m/s ²
G	Mass velocity	kg/m ² .s
h	Enthalpy	kJ/kg
$h_{c(a)}$	Assumed condensation film coefficient	W/m ² .K
$h_{c(b)}$	Calculated mean condensation film coefficient for a tube bundle	W/m ² .K
j_s	Shell-side friction factor	-
j_t	Tube-side friction factor	-
k	Thermal conductivity	W/m.K
K_1	Constant	-
l_B	Baffle spacing	mm
$LMTD$	Log mean temperature difference	°C
L_t	Length of tubes	m
m	Mass flowrate	kg/h
M	Molecular weight	kg/kmol
n_1	Constant	-
n_t	Number of tube side passes	-
N_r	Number of tubes in centre row	-
N_{tr}	Average number of tubes in a vertical tube row	-
N_T	Number of tubes	-
p_t	Tube pitch	m
P_o	Atmospheric pressure	bar
P_c	Operating pressure of the condenser	bar
ΔP	Pressure drop	
Q	Heat duty	kW
R	Factor	-
Re	Reynolds number	-
R_m	Fouling factor of condensing methanol	K.m ² /W
R_w	Fouling factor of water	K.m ² /W
S	Factor	-
t	Temperature of cold fluid	°C
\bar{t}	Mean temperature of cold fluid	°C
T_1	Inlet temperature of vapour	°C
T_c	Condensation temperature of vapour at the operating pressure of condenser	°C
\bar{T}	Mean temperature of hot fluid	°C
T_w	Mean temperature condensate	°C
T_w	Tube wall temperature	°C
ΔT_m	True temperature difference	°C
u	Velocity	m/s
U_a	Assumed overall heat transfer coefficient	W/m ² .K
U_c	Calculated overall heat transfer coefficient	W/m ² .K

Greek symbols

ρ	Density	kg/m ³
μ	Viscosity	Pa.s
Γ_h	Condensate loading on a horizontal tube	kg/s.m



Universidad de
Guayaquil

Facultad de
Ingeniería Química

INQUIDE

Ingeniería Química y Desarrollo

<https://revistas.ug.edu.ec/index.php/iqd>



ISSN – p: 1390 –9428 / ISSN – e: 3028-8533 / INQUIDE / Vol. 07 / N° 01

Subscripts

- 1 Inlet
- 2 Outlet
- L Liquid or condensate
- t Tube-side fluid
- v Vapour